ACTA NEUROBIOLOGIAE EXPERIMENTALIS

Research Paper Acta Neurobiol Exp 2015, 75: 220–237

Comparative immunohistochemical study of the effects of pilocarpine on the mossy cells, mossy fibres and inhibitory neurones in murine dentate gyrus

Norbert Károly, Endre Dobó*, and András Mihály

Department of Anatomy, Faculty of Medicine, University of Szeged, Szeged, Hungary,
*Email: dobo.endre@med.u-szeged.hu

Treatment with pilocarpine (PILO) induces variable degrees of loss of mossy cells (MCs) and mossy fibre (MF) sprouting in rodents, the relationships of which have not been examined in individual animals. Our aim was to test whether the loss of MCs and MF sprouting are coupled processes in PILO-treated rodents. Animals which exhibited intense PILO-induced convulsions for at least 30 min were used in this study. After a 2-month survival period, the incidence of epileptic seizures was checked individually by neuropeptide-Y (NPY) immunohistochemistry, and the numbers of MCs were counted by means of immunohistochemistry, for calretinin (CR) in mice and calcitonin gene-related peptide (CGRP) in rats. MF sprouting was checked by using Timm's silver-sulphide method for zinc. In our comparative studies, NPY immunohistochemistry resulted in more positive animals than on zinc staining. The CR immunoreactivity remained unchanged even in those mice that displayed MF sprouting and greatly increased NPY immunoreactivity. CR immunoreactivity was also verified after transection of the fornix to exclude the extrahippocampal source of this peptide. However, the CGRP immunoreactivity was severely reduced in those rats that exhibited simultaneous increases in zinc content and NPY immunoreactivity in the supragranular layer and stratum lucidum. Our findings suggest that the MCs survive PILO treatment in mice, but not in rats. There is direct evidence of a close relationship between the loss of MCs and MF sprouting in rats, but not in mice. Thus, similar PILO seizures may result from different changes in the neuronal circuits of rodents.

Key words: dentate gyrus, pilocarpine, mossy fibres, seizures, neuropeptide-Y, immunohistochemistry

ABBREVIATIONS

CGRP – calcitonin gene-related peptide
CR – calretinin
DAB – 3,3'-diaminobenzidine
DG – dentate gyrus
GC – granule cell
IML – internal molecular layer
IR – immunoreactive
MC – mossy cell
MF – mossy fibre
NPY – neuropeptide-Y
PB – phosphate buffer
PILO – pilocarpine
SE – status epilepticus
SGL – supragranular layer
SL – stratum lucidum
SLM – stratum lacunosum-moleculare
SRS – spontaneous recurrent seizures
Syn-I – synapsin-I
TLE – temporal lobe epilepsy

INTRODUCTION

The pilocarpine (PILO) model of epilepsy in rodents reproduces some of the features of human temporal lobe epilepsy (TLE) (Nadler et al. 1980, Turski et al. 1984, Ben-Ari 1985). A single dose of PILO acutely initiates progressive behavioural changes indicative of status epilepticus (SE), and the animals may subsequently exhibit spontaneous recurrent seizures (SRS). The acute period of SE or SRS has been reported to

Correspondence should be addressed to E. Dobó
Email: dobo.endre@med.u-szeged.hu

Received 03 October 2014, accepted 17 May 2015

cause characteristic brain damage, including neuronal loss and sprouting of the mossy fibres (MFs) in the hippocampal formation (Turski et al. 1983, Mello et al. 1993).

It is well known that the persistent and repetitive seizures in TLE may lead to hilar cell death in the dentate gyrus (DG) (Margerison and Corsellis 1966, Babb et al. 1984, Mathern et al. 1997). Mossy cells (MCs), which are a type of the principal neurones, have extensive processes to the internal molecular layer (IML) in several mammals (Buckmaster et al. 1996). Damage to the MCs, as described in both human TLE (Babb et al. 1984) and animal models (Nadler et al. 1980, Sloviter 1987), results in vacated postsynaptic sites on the granule cells (GCs), and consequently changes their synaptic outputs profoundly.

The GCs have been reported to express neuropeptide-Y (NPY) in animals that suffer from SRS (Sperk et al. 1992, Winawer et al. 2007). These neurones react to SRS with axonal sprouting, but a growing number of reports have indicated that epileptogenesis may occur without prior MF sprouting (Longo and Mello 1997, 1998). The sprouted axons may form connections, but their postsynaptic targets are obviously different, depending on their microenvironments in the CA3 region, hilum and IML (Mello et al. 1993).

The neuropeptide-Y (NPY)-expressing interneurones are also severely affected by SE (Colmers and Bahh 2003). The expression of NPY increases dramatically in the interneurones of the DG after seizures (Colmers et al. 1988, Marksteiner et al. 1990), and an elevated level of NPY has become a useful marker of epileptic activity in the DG (Scharfman and Grey 2006). The changed neuronal circuitry modifies the activities of both the excitatory and inhibitory synapses in the epileptic hippocampal formation, which is reflected by the protein compositions of the synapses.

The extent of the effects of PILO treatment on the MCs, interneurones and GCs differs considerably. Although these cells are highly interconnected, their simultaneous changes have not yet been examined. This prompted us to investigate the simultaneous changes of these cells in the same animals by means of histochemical methods. Our particular aim was to test whether the loss of MCs and MF sprouting are coupled processes in PILO-treated rodents. We assumed a positive correlation between the damage to the MCs and MF sprouting in the animals 2 months after PILO-induced SE. In order to either confirm or disprove this assumption, we applied a novel methodological approach to visualize the MCs and the ectopic MFs in the same animals.

For the detection of the MCs, their marker proteins, calretinin (CR) and calcitonin gene-related peptide (CGRP), were immunolabelled in mice (Liu et al. 1996) and rats (Freund et al. 1997), respectively. These proteins accumulated in a synaptic field within the innermost zone of the IML, which is often designated the supragranular layer (SGL). If these proteins have specific synapse-related functions, any change in the density of these markers in the SGL may reflect the activities of the MCs. Since the DG has CR-immunoreactive (IR) axons of extrahippocampal origin from the supramamillary nucleus *via* the fornix into the IML, which is responsible for the CR immunoreactivity in the IML of green monkey and rat (Borhegyi and Leranth 1997), the effect of transection of the fornix on the density of

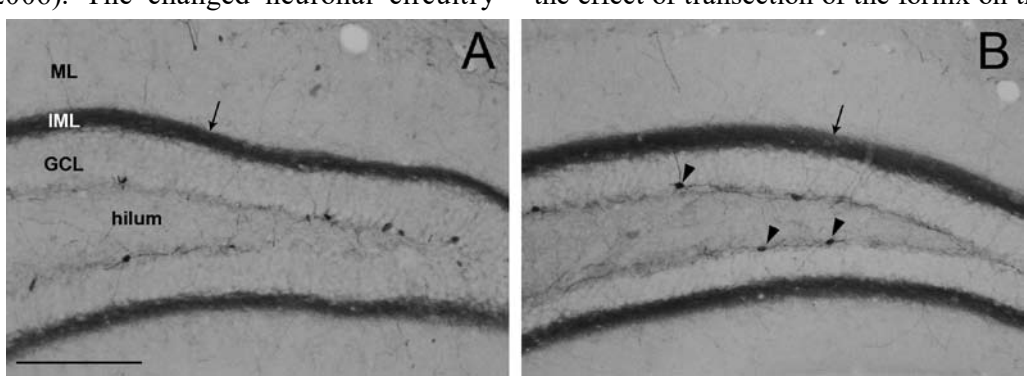

Fig. 1. No changes in CR immunoreactivity were induced by treatment with PILO in the mouse DG. Intense staining can be noted in the IMLs of both the control (A) and the PILO-responsive (B) mice (arrows). The CR-IR neurones survived the treatment (arrowheads). (GCL) granular cell layer; (IML) inner molecular layer; (ML) molecular layer. Scale bar is 150 μm (A and B).

the CR immunoreactivity in the IML was examined in a subset of our experiments.

The GCs with altered chemotype and a subset of the activated interneurones were visualized by using NPY immunohistochemistry. The MFs were demonstrated by means of zinc histochemistry (Mello et al. 1993). The presumably increased number of synaptic sites due to the sprouted MFs was revealed by synapsin-I (Syn-I) immunohistochemistry, the distribution of the Syn-I immureactivity was compared with the densities of ectopic MFs and NPY in the same PILO-treated animals. In order to achieve our aims, we elaborated a novel method, which combines immunohistochemical and zinc histochemical techniques on consecutive sections.

METHODS

Animal treatment with PILO

Totals of 97 male Wistar rats (220–300 g) and 128 male CFLP mice (25–30 g) (Animal Husbandry Services, Domaszék, Hungary) were used in this study. 83 rats and 92 mice were injected intraperitoneally (ip) with doses of PILO (Sigma-Aldrich Co., St. Louis, MO, USA) that were suitably adjusted for the species and strains so as to cause only two-thirds of the animals to exhibit SE (in order to diminish the death rate). In preliminary experiments, doses of 380 mg/kg and 190 mg/kg PILO were found to be appropriate for this purpose in rats and mice, respectively. The remaining animals displayed various levels of salivation and convulsions. With these PILO doses, approximately half of the animals that exhibited SE died on the day of treatment. Ninety minutes after SE onset, the animals were injected with diazepam (Seduxen) (Richter Gedeon, Budapest, Hungary) (10 mg/kg, ip). The control animals received the same volume of physiological saline, the solvent of PILO. The animals that developed SE during the treatment were studied, and are referred to below as PILO-treated animals.

Surgical procedure for fornix lesion

A fimbria-fornix lesion was produced in 8 anaesthetized (sodium pentobarbital (65 mg/kg body weight); Sigma-Aldrich, St. Louis, MO, USA) mice mounted in a stereotaxic apparatus. An L-shaped wire knife (0.7 mm wide) was introduced into the brain through a small hole in the skull, 0.25 mm laterally to the midline and 0.1 mm caudally to the bregma, down to 3.5 mm below the dura, and was then rotated to a distance of 0.25 mm in both directions so as to produce a lesion of the fornix according to the Mouse Brain atlas of Franklin and Paxinos (1997).

Tissue preparation

The PILO-treated and control animals were sacrificed 2 months after the injections. The animals were deeply anaesthetized with diethyl ether, and perfused through the ascending aorta with 0.3% sodium sulphide in 0.1 M phosphate buffer (PB), and then with 4% formaldehyde in PB. The brains were dissected and cryoprotected overnight in 30% sucrose in PB at 4°C. Coronal plane brain sections were cut on a freezing microtome at a thickness of 24 μm on the subsequent days following fixation. The sections for immunohistochemistry were stored in PB containing 0.1% sodium azide in a refrigerator until processing, while the sections for Timm's silver sulphide staining were mounted on glass slides (ChemMate Capillary Gap Plus Slides, DAKO A/S BioTek Solutions, USA), air-dried and stored in the dark at ambient temperature until development.

Immunohistochemistry

The sections were treated with 0.5% Triton X-100 and 3% hydrogen peroxide, and then with normal swine serum (1/10). The following primary antisera were used: rabbit anti-Syn-I (Chemicon, Temecula, CA, USA, 1/1 000), sheep anti-NPY (Peninsula Laboratories, Belmont, CA, USA, 1/48 000), goat anti-CR (Chemicon, Temecula, CA, USA, 1/2 000) and rabbit anti-CGRP (Sigma-Aldrich, St. Louis, MO, USA, 1/10 000). The sections were incubated under continuous agitation at room temperature overnight. After washing, the sections were incubated with the appropriate biotinylated secondary antibody (Jackson ImmunoResearch, West Grove, PA, USA, 1/500) for 90 min, and finally with peroxidase-labelled streptavidin (Jackson ImmunoResearch, West Grove, PA, USA, 1/1 000) for 90 min. The sites of immunoreaction were visualized with 3,3'-diaminobenzidine (DAB) in the absence of nickel for CR and in the presence of nickel for CGRP, NPY and Syn-I.

Timm's silver sulphide method

The sections were processed for Timm's staining according to Danscher and coworkers (2004). The composition of the staining solution: 60 ml of 50% gum arabic, 10 ml of 2 M sodium citrate buffer (pH 3.7), 30 ml of 5.67% hydroquinone, and 0.5 ml of 17% silver nitrate solution. The sections were continuously agitated in a dark chamber for 50–60 min. It should be noted that in our preliminary studies, a development time of 35 min revealed the zinc-containing elements in the hilum and stratum lucidum (SL) appropriately, but the expected recurrent MF sprouting into the IML was found to require 50 min in rats and 60 min in mice. The staining process was terminated with 2% sodium acetate, and the unreacted silver ions were removed with 5% sodium thiosulphate. The sections were covered with DPX mounting medium.

Visualization of the fornix lesion

The correct site of the lesion was confirmed *via* the appearance of erythrocytes extravasated from the breached blood vessels, which exhibited peroxidase-like activity. Their location was revealed by means of the brown colour of the reaction product of 0.05% DAB with 0.01% hydrogen peroxide in PB for 30 min. Thereafter, the sections were stained blue with haematoxylin for Nissl substance.

Image analysis

Pictures were taken with an image-capture system (Olympus DP50) attached to an Olympus BX-50 microscope (Soft Imaging System GmbH, Münster, Germany). Image analysis was performed with Adobe Photoshop 7 (Adobe Systems Incorporated, San Jose, CA, USA). The pixel density of immunoreactivity was measured by a researcher blind to the experimental conditions of the animals. Briefly: through use of the "marquee" tool, 8–12 circular selections 0.1 mm in diameter were made in immediately adjacent positions along the layers. The average of 10 background determinations (carried out near the layers of interest at neuropil sites not demonstrating positive staining) was subtracted from the average pixel densities measured within the hippocampal layers. Differences between the corresponding hippocampal regions of PILO-treated and control animals were assessed by using the unpaired one-tailed Student's *t* test. Data were analysed and plotted with the aid of GraphPad 4.0 (GraphPad Software, Inc, CA, USA). For every measurement, 8 hippocampal sections in the rat model and 12 sections in the mouse model were used from each animal. Pearson's correlation analyses were used to evaluate the relationship between the optical densities of NPY and Syn-I.

Cell count

The numbers of CR-IR hilar neurones were counted on 12 sections of each mouse DG, using Image-Pro Plus 4.5.1 (Media Cybernetics, Inc., USA) by a researcher blind to the experimental conditions. A cell was identified as one CR-IR neurone provided an area of at least 50 μm^2 exhibited an average pixel density of at least 60 above the background value. The total areas of DGs per mouse were summed, and the densities of CR-IR hilar neurones were determined as number per mm^2. The difference between the control and treated animals was evaluated by the unpaired one-tailed Student's *t* test.

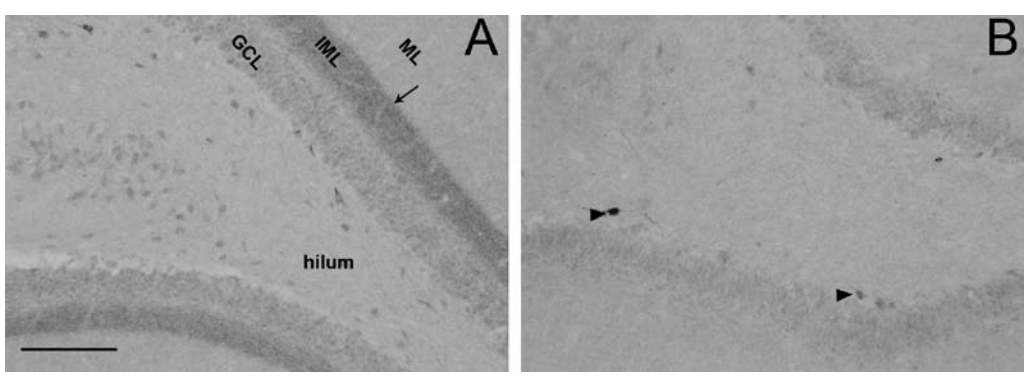

Fig. 2. Reduction in CGRP immunoreactivity in the PILO-responsive rats. In a control rat (A), the DG displays a prominent CGRP-IR IML (arrow), which vanished after PILO treatment (B). A few immunopositive hilar cells survived the treatment (arrowheads). (GCL) granular cell layer; (IML) inner molecular layer; (ML) molecular layer. Scale bar is 100 μm (A and B).

RESULTS

Effects on the mossy cells

CR immunohistochemistry and fornix lesion in mice

The CR immunoreactivity in the control mice was similar to that described by Liu and colleagues (1996). CR-IR somata and processes were seen in the DG, and a prominent IR band was observed in the IML.

The densities of CR-IR cells were compared in the control and PILO-treated animals (Fig. 1A, B). Altogether 127 and 196 CR-IR cells were identified in the control and PILO-treated mice, respectively. In terms of density values (control: 24.96 cell/mm^2; treated: 24.15 cell/mm^2), no significant change was found (P>0.05%). Representative sections were counterstained with cresyl violet for nucleus and Nissl substance. None of the counterstained sections exhibited a noticeable cell loss in the DG.

Alterations in CR immunopositivity were not encountered after PILO treatment in the IML of the dorsal DG (Fig. 1A, B). Since some authors (Borhegyi and Leranth 1997, Maglóczky et al. 2000) have postulated that a considerable number of the CR-IR processes in the IML originate from the supramamillary nucleus through the fornix, this bundle of projection fibres was transected in certain control animals in order to evaluate the proportions of the CR-IR synapses of the extra- and intrahippocampal sources. We found that fornix transection did not cause changes in the CR-IR pattern. Equally massive, homogeneous CR-IR bands were found in the IMLs on both sides (P>0.05%). Similarly, no change was detected in the densities of the CR-IR cells in the hilum (not shown).

CGRP immunohistochemistry in rats

In the control rats, the most intense staining was found in the IML, which appeared as a homogeneous band, in accordance with earlier observations (Freund et al. 1997). Moreover, various numbers of weakly stained CGRP-IR multipolar neurones were also scattered in the hilum (Fig. 2A). Labelled neuronal elements were not found outside the DG.

The PILO treatment resulted in marked changes in the CGRP immunoreactivity. The CGRP-IR staining disappeared from the IML in 69% (9/13) of the PILO-treated rats (Table I). We identified 483 and 21 CGRP-IR neurones in the hila of the control and PILO-treated rats. The number of CGRP-IR hilar neurones was reduced from 90.24 cell/mm^2 to 3.74 cell/mm^2 (4.35% of the control; P<0.05%) (Fig. 2B).

Mossy fibre sprouting

Our observations concerning the zinc-containing elements in the hippocampus are in good agreement with the literature findings (Lemos and Cavalheiro 1995, Cavalheiro et al. 1996). In the untreated animals, Timm's staining was localized in strongly stained varicose axons in the hilum (Fig. 3A, C) and in the SL. There was a weak homogeneous reaction in the IML in both rodent species. In general, this staining was found to be more constant and more intense in the rat than in the mouse. In mice, the staining density in the IML demonstrated considerable individual differences.

The animals which exhibited SE were checked for the presence of MF sprouting. Forty-one percent (7/17) of the PILO-treated mice and 54% (7/13) of the PILO-treated rats displayed massive increases in staining intensity in the hilum and the SL (Table I). The black infrapyramidal layer of region CA3 also increased in width. Moreover, dark zinc-containing varicose axons appeared within a narrow band adjacent to the GCs, i.e. the SGL, which were interpreted as ectopic MF sprouting (Fig. 3B, D). Those animals which exhibited this ectopic MF sprouting in the SGL were termed Timm-positive animals.

In the Timm-positive rats, the zinc-positive elements disappeared from the outer zone of the IML, outside the SGL (Fig. 3B). In contrast, in the Timm-positive mice, despite the presence of ectopic MFs in the SGL, the staining did not vanish from the outer zone of the IML (Fig. 3D). The fornix lesion did not change the staining pattern or the intensity of the zinc histochemistry of the mouse hippocampus on either side after a survival period of 6–7 postoperative days.

Effects on the interneurones

Moderate NPY immunostaining was found in small perikarya and their stem dendrites throughout the DG and the stratum oriens in the CA1 area of the control rats and mice, but not in the perikarya of the GCs or the pyramidal cells, in agreement with what was described earlier by Köhler and others (1986). The staining pat-

terns differed slightly between the two species (Fig. 4A, C). In the mouse, the neuropil within the layers of the DG was homogeneously and weakly punctuate (Fig. 4C). The stratum lacunosum-moleculare (SLM) displayed the highest immunoreactivity for NPY. In the rat, however, the intense staining was observed in the molecular layer where the outer strip contained the highest density of NPY-IR dots (Fig. 4A).

The NPY immunoreactivity was enhanced dramatically throughout the entire DG and the SL in both species (Fig. 4B, D). In 53% (9/17) of the PILO-treated mice (Table I) an increased NPY immunoreactivity was experienced in these areas (Fig. 4B, D), whereas in the other parts of the hippocampus, including the SLM, no marked changes were observed. The immunoreactivity for NPY also increased in the molecular layer, but to a much lesser extent than in the areas of MFs (Fig. 4D). Characteristically, one band that seemed slightly narrower than the IML, i.e. the SGL, stood out from the homogeneously labelled plexiform layer in 41% (7/17) of the PILO-treated mice (Table I). The strong staining often concealed the NPY-IR neurones in the MF-containing areas. However, in those hippocampal areas where the MFs were not present, the NPY-IR perikarya were labelled much more intensely than those in the control mice.

The treatment with PILO resulted in similar changes in the rat hippocampus. The NPY staining sharply demarcated the MF-containing hilum and SL in 69% (9/13) of the PILO-treated rats (Table I). The SGL was also revealed by NPY immunohistochemistry in 54% (7/13) of the PILO-treated rats (Table I).

Comparative analysis of the effects of PILO on the mossy cells, mossy fibres and interneurones in mice and rats

Mice

Whereas no changes were observed in the CR immunostaining of the mouse DG, marked enhancements were found in the density of MFs and the NPY immuno-

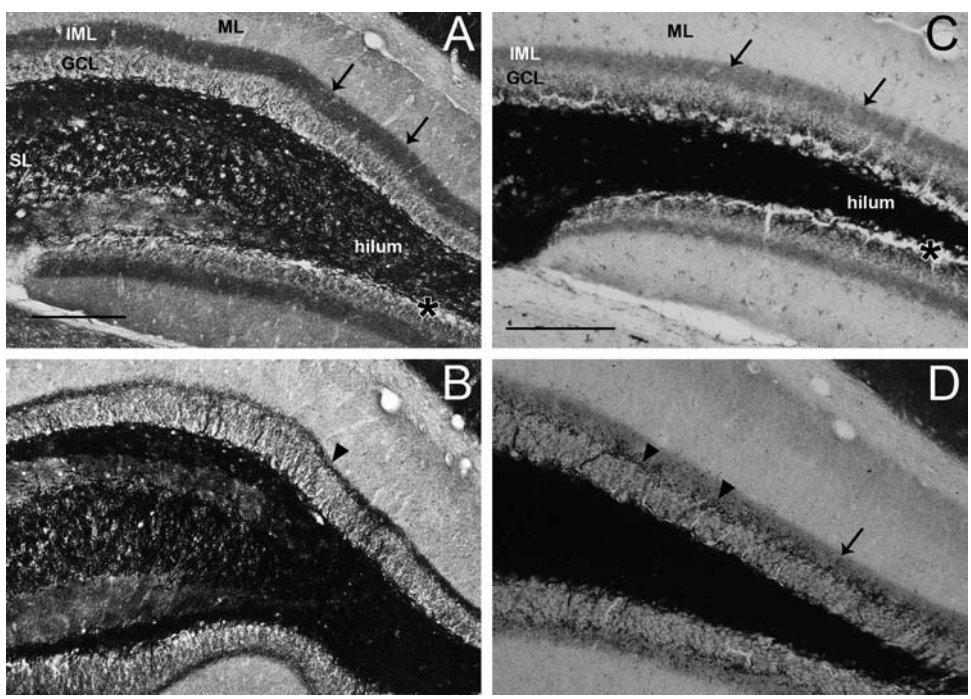

Fig. 3. Ectopic sprouting of MFs is induced by PILO treatment, as evidenced by Timm's staining. The hilum exhibits the highest density of zinc, and a distinct IML (arrows) is seen in the control animals (rat – A, mouse – C). In the PILO-responsive rats, the staining in the outer two-thirds of the IML has disappeared, while the zinc content remains in its inner one-third (i.e. the SGL) (arrowhead in B). In the PILO-responsive mice, the staining has not vanished in the IML (arrow in D), while the labelling in the SGL is enhanced (arrowhead in D). Artificial shrinkage is visible (asterisks in A and C). (GCL) granular cell layer; (IML) inner molecular layer; (ML) molecular layer; (SL) stratum lucidum. Scale bars are 100 μm (A and B) and 150 μm (C and D).

reactivity (Table I). In summary, one-fifth more animals displayed alterations in the NPY immunoreactivity than in Timm's staining (53% vs. 41%). Among those individuals that showed any changes in either Timm's staining (7/17) or NPY immunostaining (9/17), 6 animals (6/17) displayed similar changes, i.e. double positivity for the ectopic appearance of zinc and NPY in the SGL. Two mice exhibited opposite changes in the SGL: one Timm-positive mouse was negative for a NPY-IR SGL (though the immunoreactivity was increased in the hilum and the SL) (see mouse #7 in Table I) and one Timm-negative mouse (i.e. without ectopic MF sprouting) was positive for a NPY-IR SGL (see mouse #2 in Table I).

Rats

Paired comparisons of the CGRP and NPY immunohistochemistry and the Timm's staining (Table I) resulted in a one-to-one correlation between a negative CGRP-IR IML (9/13) and a considerable enhancement of the NPY immunoreactivity in the SL (9/13) (Table I). However, the negativity of the CGRP-IR IML did not coincide with the unambiguous change in Timm's staining, i.e. in the SGL (7/13) (Table I). It is noteworthy that every Timm-positive animal exhibited a loss of CGRP immunoreactivity from the IML. Comparison of the Timm's staining with the immunohistochemistry for NPY yielded results in agreement with those for CGRP; each Timm-positive animal exhibited a dramatic change in density of the NPY immunoreactivity in the SL. In 2 Timm-positive animals (2/7), the SGL was found to be positive, but contained no enhanced NPY immunoreactivity in this layer, in spite of the strongly IR hilum and SL (see rats #3 and 7 in Table I). Interestingly, 2 rats with an NPY-IR SGL proved to be Timm-negative.

Syn-I immunohistochemistry

Strong immunoreactivity for Syn-I was found in the MFs in both rodent species. The cell bodies were not labelled. The molecular layer was moderately positive (Fig. 5A, C).

In the mice, after survival for 2 months, the density of labelled elements in the SL was increased

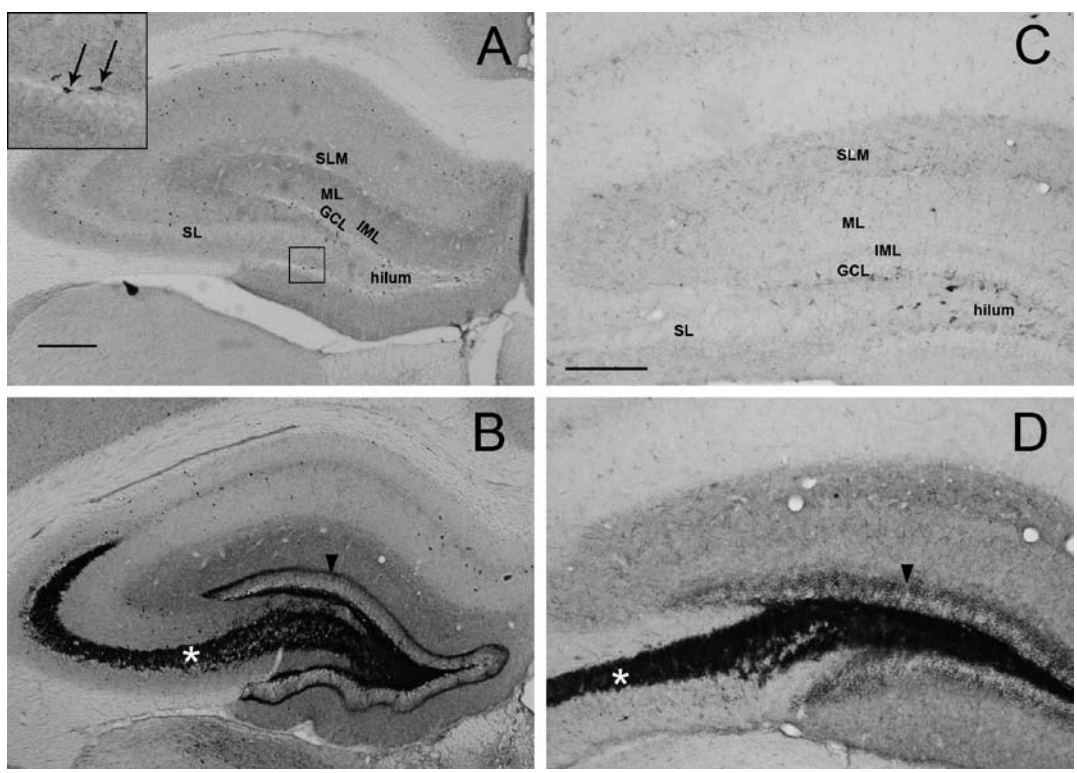

Fig. 4. PILO treatment increased the NPY immunoreactivity to a great extent in the rodent hippocampi. In the control sections (rat – A, mouse – C), the immunoreactivity is mainly confined to the cell bodies and larger processes (arrows in A inset). In the PILO-responsive animals (rat – B, mouse – D), the NPY immunoreactivity was dramatically increased in the SL (asterisks) and hilum, and moderately in the SGL (arrowhead). Scale bars are 250 μm (A and B) and 200 μm (C and D).

Table I

Comparative qualitative analysis of the effects of PILO on the densities of the synaptic fields of MCs, MFs and interneurones in the DGs of mice and rats

Mouse #	CR[1]	Timm[2]	NPY	Rat #	CGRP[1]	Timm[2]	NPY	Syn-I
1	ND	+ (weak)	+[2,3,4]	1	-	+	+[2,3,4]	+[2(weak),3,4]
2	ND	-	+[2,3,4]	2	-	+	+[2,3]	+[2,3,4]
3	ND	+	+[2,3,4]	3	-	+	+[3,4]	+[3,4]
4	ND	-	-	4	-	+	+[2,3,4]	+[3,4]
5	ND	+	+[2,3,4]	5	-	+	+[2,3,4]	+[2(weak),3,4]
6	ND	-	-	6	-	-	+[2,3,4]	+[2,3,4]
7	ND	+ (weak)	+[3,4]	7	-	+ (weak)	+[3,4]	+[3,4]
8	ND	-	-	8	ND	-	-	-
9	ND	-	+[3]	9	ND	-	-	-
10	ND	-	-	10	-	+	+[2,3,4]	+[2,3,4]
11	ND	+	+[2,3,4]	11	ND	-	-	-
12	ND	-	-	12	-	-	+[2,3,4]	+[2(weak),3,4]
13	ND	-	-	13	ND	-	-	-
14	ND	-	-		9/13 69%)	7/13 54%)	9/13 69%)	9/13(69%)
15	ND	+	+[2,3,4]	1: in IML				
16	ND	-	-	2: enhanced IR in SGL				
17	ND	+	+[2,3,4]	3: enhanced IR in SL				
		7/17 41%)	9/17 53%)	4: enhanced IR in hilum				
				ND: no detected changes				

No loss of CR-IR cells (presumably MCs) or fibres was detected in mice after PILO treatment. In contrast, a considerable loss of CGRP-IR cells (presumably MCs) and IML was observed in 69% of the PILO-treated rats. 41% and 54% of the PILO-treated mice and rats, respectively, exhibited dramatic increases in Timm's staining in the SGL, while 53% and 69% of the PILO-treated mice and rats displayed dramatically enhanced NPY immunoreactivity throughout the entire DG and the SL, respectively. In both species, the paired comparisons revealed some animals which manifested opposite changes in the SGL, i.e. Timm+/NPY- and Timm-/NPY+ bands. A one-to-one correlation was found between the absence of CGRP-IR synaptic field in the IML and the upregulation of the NPY-IR elements. Whereas individual variability in NPY immunoreactivity was observed, its great enhancement in the SL (see NPY+3) was a standard phenomenon in the PILO-responsive animals, and might serve as a reliable marker of a substantial change in the neural circuits. Increases in Syn-I and NPY immunoreactivity were seen in parallel in the PILO-responsive rats. Such a coincidence was not observed in the mice. (ND) no detectable changes; (Timm+) appearance of zinc-containing ectopic fibres in the SGL; (1) in the IML; (2) enhanced NPY-IR in the SGL; (3) enhanced NPY-IR in the SL; (4) enhanced NPY-IR in the hilum.

significantly in the Timm-positive animals, as described by Károly and coauthors (2011). Moreover, the layer displaying Syn-I immunostaining thickened considerably. The dentate hilum, which contains strongly-stained MF terminals, as verified by Timm's staining, displayed a highly significant drop in Syn-I staining intensity. In the IML, the overall staining did not change significantly (Fig. 5C).

Analysis of the brain sections from PILO-treated and control rats revealed similarities and differences as compared with the mice. The PILO-induced seizures enhanced the Syn-I immunoreactivity significantly in every layer (Fig. 5B) in 69% (9/13) of the PILO-treated rats, including the hilum, which exhibited much weaker immunolabelling in the mice (Fig. 5B, D). Syn-I immunoreactivity of various intensity additionally appeared in the SGL of 46% (6/13) of the treated rats, which was not stained in the controls.

Correlation analysis between NPY and Syn-I immunoreactivities

Since the PILO treatment changed the NPY and Syn-I immunoreactivities in the same layers in both species, the possibility of a correlation between these elevated densities was probed in the affected areas in the individual animals. The data for semiquantitative analysis were collected from paired adjacent sections, the members of which were immunostained for NPY and Syn-I, respectively (Fig. 6).

In the mice, positive correlations were found between the two markers in the SL (R^2 Linear =0.759, P<0.05). The increased density of the NPY immunoreactivity was inversely proportional to the density of Syn-I in the hilum (R^2 Linear =0.832, P<0.05) (Fig. 7C, D).

In the rats, positive proportional changes were found between the markers in the SL (R^2 Linear =0.535, P<0.05) and in the hilum (R^2 Linear =0.542, P<0.05) (Fig. 7A, B).

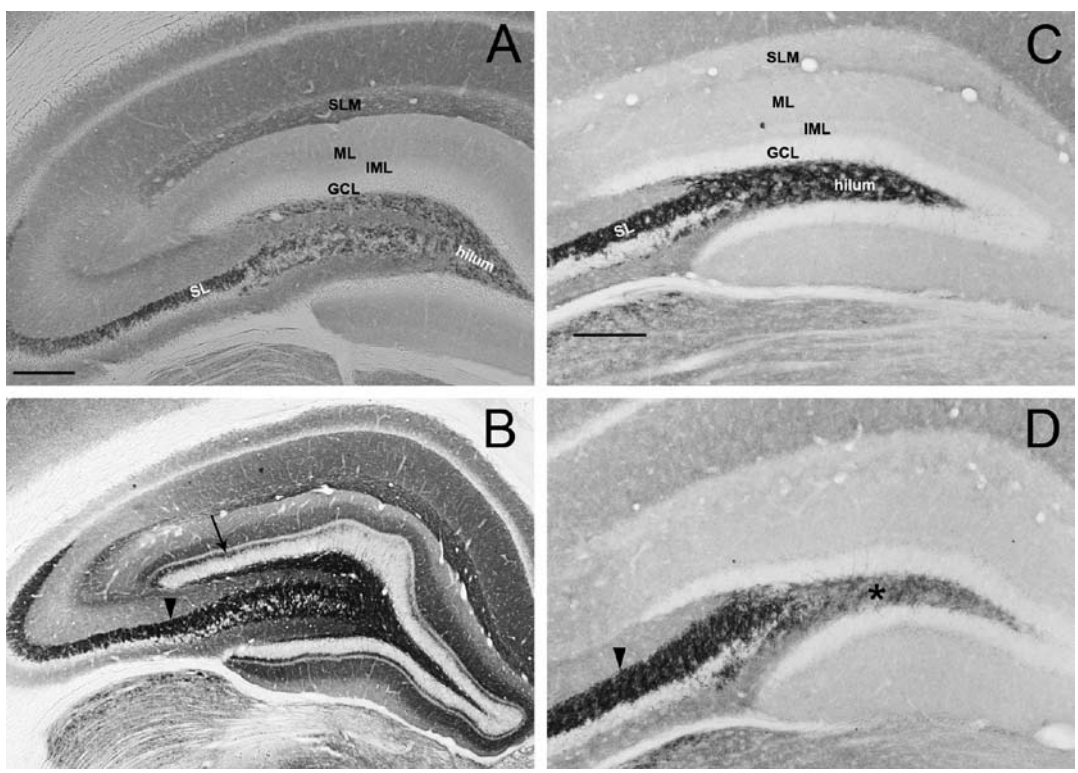

Fig. 5. Species-dependent changes in Syn-I immunoreactivity in the PILO-responsive rodents. Similar distributions of Syn-I are found in the control rat (A) and mouse (C) hippocampi. In the rat, all the layers of the synaptic fields display increases to various extents in Syn-I immunoreactivity. The most characteristic increase is found in the SGL (arrow in B). In both the mouse and the rat, significantly enhanced immunoreactivity is seen in the SL (arrowheads), but a decrease is noted in the hilum of the PILO-responsive mouse (asterisks in D). (GCL) granular cell layer; (IML) inner molecular layer; (ML) molecular layer; (SL) stratum lucidum; (SLM) stratum lacunosum-moleculare. Scale bars are 250 μm (A and B) and 200 μm (C and D).

Although the frequent coincidence of the NPY and Syn-I immunoreactivities in the SGL suggested a close relationship between these markers, our semiquantitative analysis did not indicate a correlation in this narrow band (R^2 Linear = 0.023, P>0.05). However, the paired comparisons of the subsequent sections immunostained for NPY and Syn-I revealed that all 6 animals which exhibited Syn-I immunoreactivity in the SGL were also immunopositive for NPY, as well (Table I). Only 4 of the 6 animals were found to exhibit Timm positivity in the SGL (Fig. 8).

DISCUSSION

Mossy cells

Loss of the MCs has generally been accepted as coincident with the hyperexcitability of the GCs to undergo spontaneous repetitive bursts (Sloviter 1991, Buckmaster and Jongen-Rélo 1999, Longo et al. 2003). The "dormant basket cell" theory (Sloviter 1991) hypothesized that the GABAergic basket cells lose their major source of excitatory input from the MCs, leading to disinhibition of their targets, i.e. the GCs. However, this theory is not widely accepted as it has been demonstrated that at least a subset of the MCs are able to survive PILO-induced seizures (Scharfman et al. 2001, Seress et al. 2009).

Surviving mossy cells and the mossy fibres in mice

No noticeable change was observed in the number or distribution of the CR-IR hilar perikarya (Fig. 3), 96% of which have been estimated to be MCs (Liu et al. 1996, Blasco-Ibanez and Freund 1997). No apparent reduction in the density of CR-IR synaptic elements in the IML was detected in the PILO-treated DG. The lack of any decrease in the CR immunoreactivity in the IML, and the possible extrapolation from the experimental data on monkeys and rats (Nitsch and Leranth 1993) to mice regarding whether the IML may

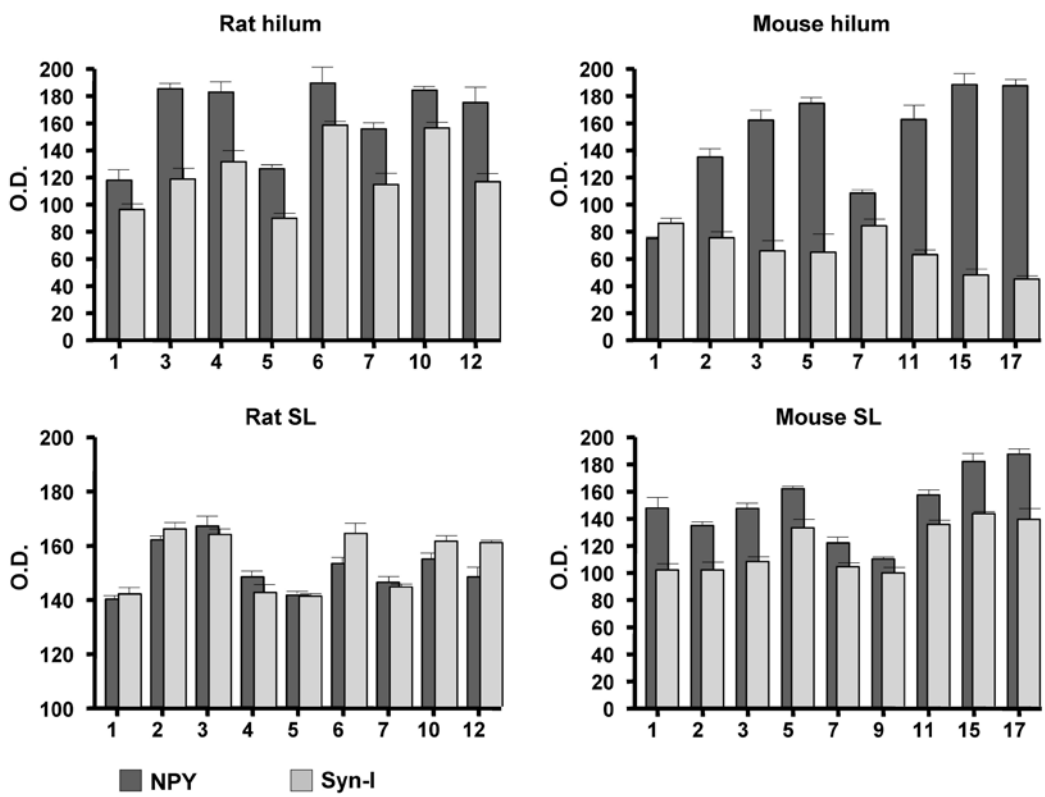

Fig. 6. Comparison of the changes in NPY and Syn-I immunoreactivities in the hilum and SL of the individual animals after PILO treatment. The numerals on the horizontal axes are the identification numbers of the animals used in the study (cf. the upper indices such as 2, 3 and 4 in Table I). The optical density values (OD) were obtained by reduction of the values of the individual PILO-treated rodents from the average values of the controls. The PILO-treated individuals with unchanged immunoreactivity were not included in the graphs. The results of Pearson's correlation analyses are shown in Fig. 7.

contain dense connections from the supramamillary nucleus, prompted us to transect the fornix unilaterally to learn whether the unaffected supramamillary axons conceal the assumed loss of axons of the MCs. The lack of changes after the fornix lesion proved that the vast majority of the staining in the IML could be ascribed to the MCs, and not to the supramamillo-hippocampal pathway in the mouse.

Our present findings are in sharp contrast with the general and widely accepted concept that the MCs are highly vulnerable to glutamate-mediated seizures. SE induced by convulsants such as PILO (Silva and Mello 2000) and kainate (Volz et al. 2011) led to a loss of MCs. In a study with two mouse strains (Balb/c and NMRI) lacking documented common ancestors (Beck et al. 2000) with the CFLP strain used here, we also

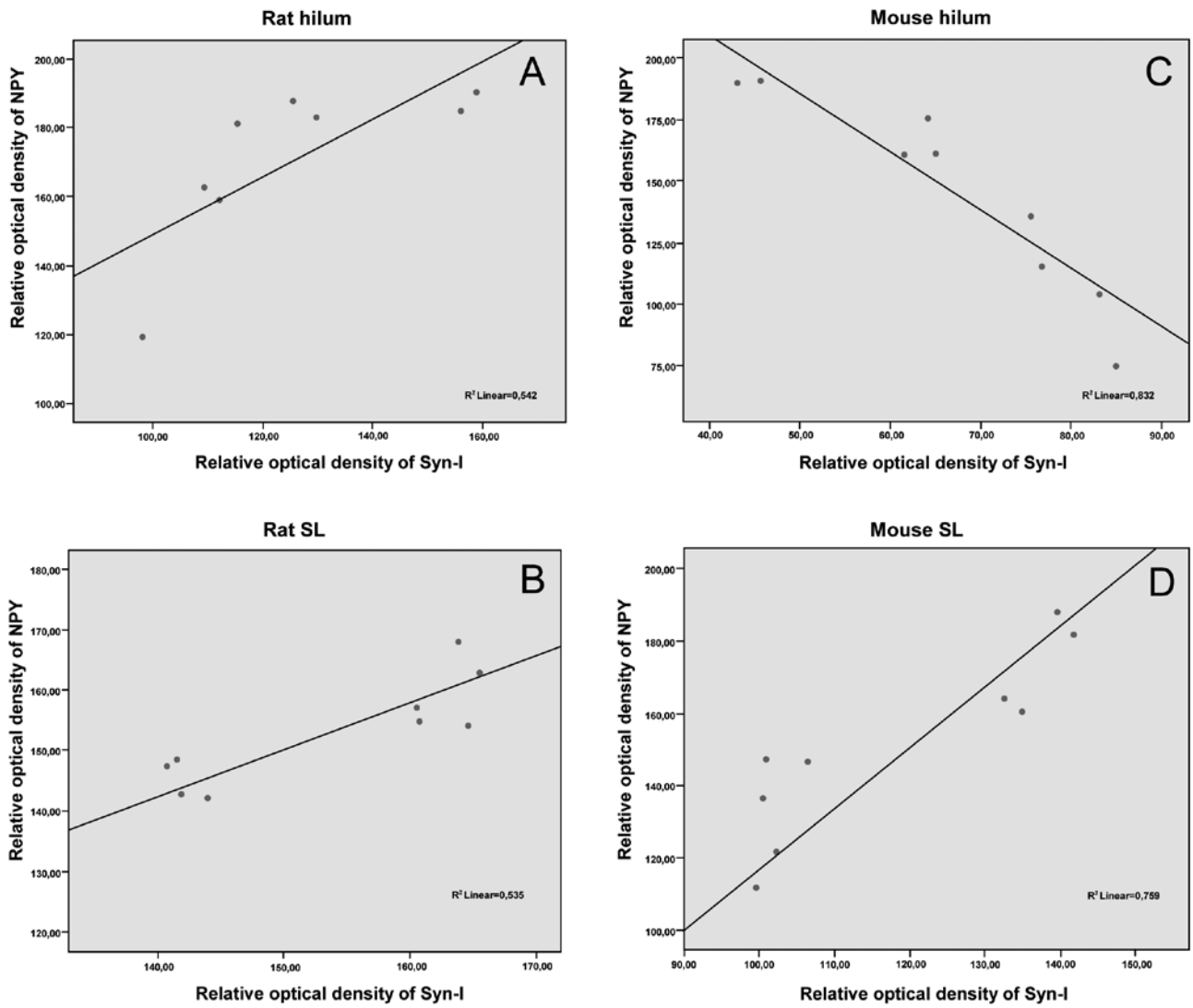

Fig. 7. Correlation analysis of the changes in NPY and Syn-I immunoreactivities induced by PILO treatment revealed a species difference between the rat and the mouse. The original data are shown in Fig. 6. The plotted data are derived from those PILO-responsive animals which displayed enhanced immunoreactivities in the hilum and SL, as indicated by the upper indices in Table 1. In the rat, positive proportional changes were found between the two markers in the hilum (R^2 Linear =0.542) (A) and SL (R^2 Linear =0.535) (B). However, in the mouse, the density of the immunoreactivity for NPY was inversely proportional to that for Syn-I in the hilum (R^2 Linear =0.832) (C), while a positive correlation was also measured in the SL (R^2 Linear =0.759) (D). (GCL) granular cell layer; (IML) inner molecular layer; (ML) outer molecular layer; (SL) stratum lucidum; (SLM) stratum lacunosum-moleculare. Scale bars are 150 µm (A and B) and 200 µm (C and D).

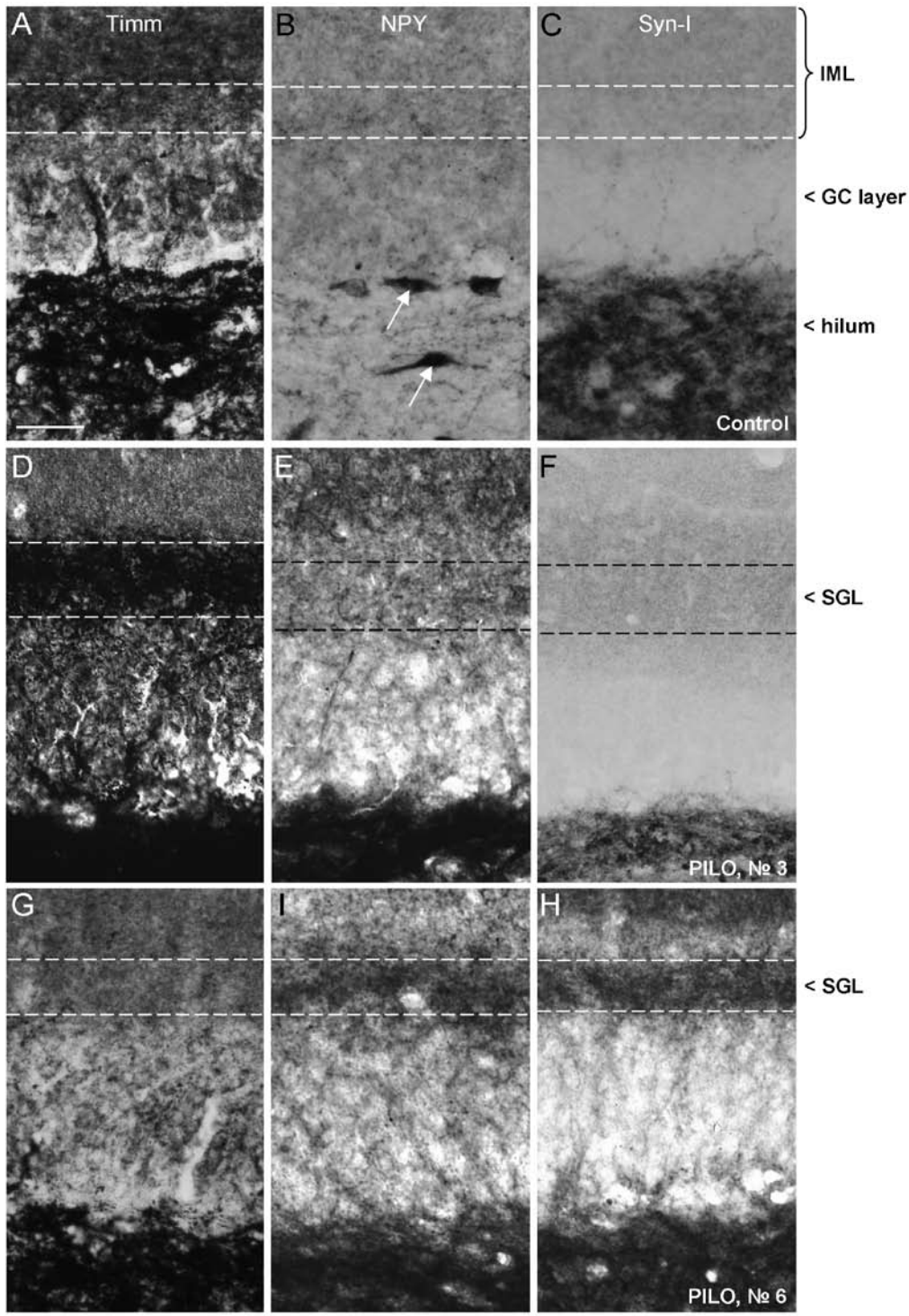

Fig. 8. Different ectopic fibres appeared in the SGL after PILO treatment. SGLs (outlined by dashed lines) of control (A-C) and PILO-treated rats #3 (D-F) and #6 (G-I) are compared after Timm's staining (A, D and G), and NPY (B, E and I) and Syn-I immunohistochemistry (C, F and H). PILO treatment resulted in "triple positive" SGL in 38% of the animals. Rat #3 displayed strong Timm-positive MF sprouting (D), but no NPY (E) and Syn-I (F) immunoreactivities in the SGL. In contrast, rat #6 showed no Timm staining (G), but intense NPY (H) and Syn-I-IR (I) puncta in the SGL. Some NPY-IR perikarya (arrows) stand out from the hilum in the control rat (B). The GCs remained unstained with the antibodies even in the intensely PILO-responsive animals (E–F, H–I). Scale bar is 50 μm.

found dramatic and different reductions in the density of the MCs after PILO treatment (Dobó et al. 2015).

Our zinc histochemistry findings corroborate the earlier literature data on the increased density of MFs in PILO-treated animals and the appearance of ectopic MFs in the SGL (Lemos and Cavalheiro 1995, Cavalheiro et al. 1996, Jiao and Nadler 2007, Polli et al. 2014). Similar distribution patterns of the zinc-containing elements were found in the control and the Timm-positive animals, which correlated with the CR immunohistochemistry. The only slight, but still noteworthy difference was the persistence of Timm's staining in the outer zone of the IML of the Timm-positive mice (Fig. 3D). The persistence of the zinc content of the layer indicates survival of the MCs (Buckmaster et al. 1992, 1996). This seems to be contradictory to the findings that PILO-induced epileptic seizures eliminated the CR-IR axons=from the IML (Silva and Mello 2000).

In summary, our experiments indicate that the MCs of the CFLP mouse may not be as vulnerable as expected in the PILO-induced SE. This is implicitly confirmed by no reduction in the numbers of (1) CR-IR perikarya in the hilum, (2) CR-IR axons in the IML and (3) zinc-containing elements in the IML, and (4) a lack of noticeable CR-IR input through the fornix.

Loss of mossy cells and mossy fibres in rats

Only a few slightly labelled CGRP-IR cells remained in the DG in the PILO-treated rats, and the immunoreactivity vanished from the IML. Although the strain-specific vulnerability of the MCs was earlier studied in mice (Dobó et al. 2015), no data on such strain differences have previously been described in rats.

The application of CGRP immunohistochemistry and Timm's staining on consecutive sections from control rats pointed to similar layers with comparable widths in the IML. The pale zinc staining in the IML could therefore be attributed to the axon varicosities of the glutamatergic MCs (Buckmaster et al. 1996, Ito et al. 2012). In all the Timm-positive rats, in which ectopic MFs appeared in the IML as a narrow band (i.e. the SGL), the Timm-positive staining indicative of glutamatergic neurotransmission vanished from the remainder of the IML (Fig. 3B), and the CGRP immunoreactivity disappeared from its whole width. Even if the MCs had survived the seizures, therefore they would have been converted into silent neurones.

Increased NPY immunoreactivity

Marked changes in the hippocampal distribution of NPY in PILO-treated species were reported by Lurton and Cavalheiro (1997), Nadler and coauthors (2007), Scharfman and Gray (2006), Winawer and colleagues (2007) and Xu and others (2014): intense staining in the synaptic fields of the MFs, i.e. the hilum and SL, and variable immunoreactivity in the SGL.

Two major sources of the elevated NPY level may be supposed. (1) The *de novo* synthesis of NPY mRNA and NPY has been reported in the GCs (Gall et al. 1990, McCarthy et al. 1998). Several experiments have shown that the tonic-clonic seizures evoked by electrical kindling (Rizzi et al. 1993), kainate (Sperk et al. 1992, Gruber et al. 1994) and PILO (Lurton and Cavalheiro 1997) result in strong NPY immunoreactivity in the MF field which persists for months. (2) NPY and its mRNA levels are also markedly increased in the hippocampal interneurones (Gall et al. 1990, Marksteiner et al. 1990, Sperk et al. 1992, Elbrond-Bek et al. 2014).

Detailed investigations have revealed that the two cell groups with elevated NPY demonstrate different time-course changes following the SE. In the study by Gruber and coworkers (1994), both cell groups reacted to the kainate-evoked SE with the rapid expression of NPY mRNA, but whereas the NPY mRNA level soared to ~60-fold in the GCs after 24 h, that in the hilar interneurones increased only 2-fold. During the next 24 h, the level of NPY mRNA in the GCs dropped to that in the control cells, while the NPY mRNA increased further in the hilar interneurones. Four months after the SE, the NPY mRNA remained at a very low level in the GCs, while that in the interneurones had continued to rise to more than 10 times the control level.

All earlier papers on the changes in limbic NPY after convulsions ascribed the increased levels of NPY in the hilum, the SL and the SGL directly to the activated GCs. Strikingly, NPY immunoreactivity within the GCs was not described at any examined time point of the post-treatment period in any of the papers, in contrast with that in the interneurones, which was observed to be intense.

Several types of NPY-IR interneurones have been distinguished in the DG (Deller and Léránth 1990). Later, others (Acsády et al. 1998, Baude et al. 1993) described nerve cells which were GABAergic and colocalized NPY and somatostatin. These cells pos-

sessed horizontal dendrites studded with a large number of spines, and were therefore referred to as spiny GABAergic cells (Acsády et al. 1998). These interneurones were classified by Gulyás and colleagues (2003) as hippocamposeptal neurones. Although NPY immunohistochemistry was not applied, the same cell type was possibly further characterized by Takács and others (2008) as a group of GABAergic neurones which exhibit densely-spiny horizontal dendrites restricted to the hilum and SL, and which establish synapses in the septum. They coined this cell type "densely-spiny hippocampal cells projecting to the medial septum". Although the neuropeptide contents of these cells are not yet known, they might also contribute strongly to the dramatic increase in NPY immunoreactivity in the hilum and SL of the chronic Timm-positive animals.

In view of the general inhibitory functions of NPY as a neuromodulator substance on the postsynaptic cells, the synergistic actions of GABA and co-released NPY are highly, though not totally protective for the principal neurones, since epileptogenesis does not seem to be a stoppable process, and progression of the spontaneous seizures results in neuronal loss.

Analogously to the appearance of NPY immunoreactivity in the SL, the newly appeared NPY immunostaining in the SGL could not be explained by the ectopic MF sprouting of the activated GCs. Direct evidence is not yet available, but the new staining could be attributable to hilar interneurones, in which the seizures could induce axonal sprouting into the SGL to establish inhibitory connections either on the proximal dendrites or on the ectopic MFs of the GCs. Indeed, ectopic sprouting of GABAergic interneurones into the SGL has been reported in the mouse model of TLE (Zhang et al. 2009).

Mossy fibre sprouting *versus* enhanced NPY as markers for epileptogenesis

The role of MF sprouting in epileptogenesis has also been debated, since spontaneous recurrent seizures were evoked without the appearance of MF sprouting in the PILO model of epilepsy and the kainate model of TLE (Longo and Mello 1997, 1998). Nevertheless, most researchers seem to agree that MF sprouting, and especially ectopic MF sprouting in the SGL, is a prerequisite for recurrent spontaneous convulsions, and Timm's staining has often been used as morphological evidence of ongoing epileptogenesis.

Robust upregulation of hippocampal NPY is an accepted marker for seizures (Sperk et al. 1992, Vezzani et al. 2002, Vezzani and Sperk 2004, Botterill et al. 2014). Our comparative studies of Timm's staining and NPY immunohistochemistry indicated that zinc histochemistry failed to highlight animals which may have undergone spontaneous convulsions.

Species-dependent changes in the levels of Syn-I

The synapsins are thought to be important molecules in synaptic maturation and in the regulation of the release of neurotransmitters (Greengard et al. 1993). On the assumption of the excessive activities of the neurones in SE animals, an increased Syn-I density was speculated in their hippocampi, and especially in the synaptic fields of the sprouted MFs.

Interestingly, the genetic deletion of Syn-I in mice led to a severe epileptic phenotype with recurrent seizures by the age of ~2 months (Baldelli et al. 2007). In those Syn-I knock-out animals, the number of synaptic vesicles containing either Glu or GABA was decreased, which supports the view that Syn-I may play a controversial role in the susceptibility to epileptic seizures (Chiappalone et al. 2009). The impairment in GABAergic inhibitory transmission was apparently more profound in epileptic seizures than that in the excitatory neuronal mechanisms (Terada et al. 1999, Baldelli et al. 2007).

Contrasting changes in Syn-I immunoreactivity were found in the three major MF areas of the PILO-treated mice. An increase in Syn-I density in the SL is in line with increases in both Timm's staining and NPY immunoreactivity.

The decrease in Syn-I density in the mouse hilum was unexpected. This reduction implies that a subset(s) of either or both of the major opposite neurotransmission systems was/were downregulated or even lost. Since the Timm's staining and the NPY immunoreactivity, indicative of the glutamatergic and a subset of the GABAergic neurones, respectively, were increased, the decrease in Syn-I density in the hilum indicates that an NPY-lacking subset of hilar GABAergic neurones (Acsády et al. 1997) could be more severely affected by PILO treatment than the other neurones.

In contrast with the mice, in the rats the PILO treatment increased the Syn-I density in all the hippocampal areas where the NPY immunoreactivity was elevated. These changes correlated positively. The increased density of Syn-I lagged significantly behind

that of NPY, which is a further indication of the ambiguous changes in the two major opposite neurotransmitter systems during epileptogenesis, and the possibly increased NPY-mediated transmission may not utilize Syn-I.

CONCLUSIONS

The DGs in PILO-treated rats and mice were compared by means of a novel combination of histochemistry for zinc and immunohistochemistry for certain neuronal markers.

The results revealed important species differences in response to epileptogenic stimuli, which should be taken into account when the experimental results obtained on one species are extrapolated to another.

In contrast with rats, the MCs were found to be unaffected in mice. Instead, a subpopulation of hilar GABAergic cells that may lack NPY appears to be more vulnerable.

The NPY-containing neurones demonstrated potential compensatory actions both for the increased excitatory MF sprouting in both species and for the lost inhibitory cells in mice, which indicates the possible roles of NPY-IR neurones in epileptogenesis.

Our results indicated that NPY immunohistochemistry may be more sensitive and reliable than Timm's staining for revelation of the epileptic processes in the chronic PILO model of TLE.

ACKNOWLEDGEMENTS

Grant: TÁMOP 4.2.2-A-11/1/KONV-2012-0052. The authors would like to thank Dr. Ibolya Török for providing critical comments on the manuscript. Special thank goes to Dr. David Durham to proofread and correct the English of the manuscript.

REFERENCES

Acsady L, Katona I, Gulyas AI, Shigemoto R, Freund TF (1997) Immunostaining for substance P receptor labels GABAergic cells with distinct termination patterns in the hippocampus. J Comp Neurol 378: 320–336.

Acsady L, Kamondi A, Sik A, Freund T, Buzsaki G (1998) GABAergic cells are the major postsynaptic targets of mossy fibers in the rat hippocampus. J Neurosci 18:3386-3403.

Babb TL, Brown WJ, Pretorius J, Davenport C, Lieb JP, Crandall PH (1984) Temporal lobe volumetric cell densities in temporal lobe epilepsy. Epilepsia 25: 729–740.

Baldelli P, Fassio A, Valtorta F, Benfenati F (2007) Lack of synapsin I reduces the readily releasable pool of synaptic vesicles at central inhibitory synapses. J Neurosci 27: 13520–13531.

Baude A, Nusser Z, Roberts JD, Mulvihill E, McIlhinney RA, Somogyi P (1993) The metabotropic glutamate receptor (mGluR1 alpha) is concentrated at perisynaptic membrane of neuronal subpopulations as detected by immunogold reaction. Neuron 11: 771–787.

Beck JA, Lloyd S, Hafezparast M, Lennon-Pierce M, Eppig JT, Festing MF, Fisher EM (2000) Genealogies of mouse inbred strains. Nat Genet 24: 23–25.

Ben-Ari Y (1985) Limbic seizure and brain damage produced by kainic acid: mechanisms and relevance to human temporal lobe epilepsy. Neuroscience 14: 375–403.

Blasco-Ibanez JM, Freund TF (1997) Distribution, ultrastructure, and connectivity of calretinin-immunoreactive mossy cells of the mouse dentate gyrus. Hippocampus 7: 307–320.

Borhegyi Z, Leranth C (1997) Distinct substance P- and calretinin-containing projections from the supramammillary area to the hippocampus in rats; a species difference between rats and monkeys. Exp Brain Res 115: 369–374.

Botterill JJ, Guskjolen AJ, Marks WN, Caruncho HJ, Kalynchuk LE (2014) Limbic but not non-limbic kindling impairs conditioned fear and promotes plasticity of NPY and its Y2 receptor. Brain Struct Funct [Epub ahead of print].

Buckmaster PS, Jongen-Relo AL (1999) Highly specific neuron loss preserves lateral inhibitory circuits in the dentate gyrus of kainate-induced epileptic rats. J Neurosci 19: 9519–9529.

Buckmaster PS, Strowbridge BW, Kunkel DD, Schmiege DL, Schwartzkroin PA (1992) Mossy cell axonal projections to the dentate gyrus molecular layer in the rat hippocampal slice. Hippocampus 2: 349–362.

Buckmaster PS, Wenzel HJ, Kunkel DD, Schwartzkroin PA (1996) Axon arbors and synaptic connections of hippocampal mossy cells in the rat in vivo. J Comp Neurol 366: 271–292.

Cavalheiro EA, Santos NF, Priel MR (1996) The pilocarpine model of epilepsy in mice. Epilepsia 37: 1015–1019.

Chiappalone M, Casagrande S, Tedesco M, Valtorta F, Baldelli P, Martinoia S, Benfenati F (2009). Opposite changes in glutamatergic and GABAergic transmission underlie the diffuse hyperexcitability of synapsin I-deficient cortical networks. Cereb Cortex 19: 1422–1439.

Colmers WF, El Bahh B (2003) Neuropeptide Y and epilepsy. Epilepsy Curr 3: 53–58.

Colmers WF, Lukowiak K, Pittman QJ (1988) Neuropeptide Y action in the rat hippocampal slice: site and mechanism of presynaptic inhibition. J Neurosci 8: 3827–3837.

Danscher G, Stoltenberg M, Bruhn M, Sondergaard C, Jensen D (2004) Immersion autometallography: histochemical in situ capturing of zinc ions in catalytic zinc-sulfur nanocrystals. J Histochem Cytochem 52: 1619–1625.

Deller T, Leranth C (1990) Synaptic connections of neuropeptide Y (NPY) immunoreactive neurons in the hilar area of the rat hippocampus. J Comp Neurol 300: 433–447.

Dobó E, Török I, Mihály A, Károly N, Krisztin-Péva B (2015) Interstrain differences of ionotropic glutamate receptor subunits in the hippocampus and induction of hippocampal sclerosis with pilocarpine in mice. J Chem Neuroanat 64–65: 1–11.

Elbrond-Bek H, Olling JD, Gotzsche CR, Waterfield A, Wortwein G, Woldbye DP (2014) Neuropeptide Y-stimulated [(35) S]GTPgammas functional binding is reduced in the hippocampus after kainate-induced seizures in mice. Synapse 68: 427–436.

Franklin KBJ, Paxinos G (1997) The Mouse Brain in Stereotaxic Coordinates. Academic Press, San Diego, CA, USA.

Freund TF, Hajos N, Acsady L, Gorcs TJ, Katona I (1997) Mossy cells of the rat dentate gyrus are immunoreactive for calcitonin gene-related peptide (CGRP). Eur J Neurosci 9: 1815–1830.

Gall C, Lauterborn J, Isackson P, White J (1990) Seizures, neuropeptide regulation, and mRNA expression in the hippocampus. Prog Brain Res 83: 371–390.

Greengard P, Valtorta F, Czernik AJ, Benfenati F (1993) Synaptic vesicle phosphoproteins and regulation of synaptic function. Science 259: 780–785.

Gruber B, Greber S, Rupp E, Sperk G (1994) Differential NPY mRNA expression in granule cells and interneurons of the rat dentate gyrus after kainic acid injection. Hippocampus 4: 474–482.

Gulyas AI, Hajos N, Katona I, Freund TF (2003) Interneurons are the local targets of hippocampal inhibitory cells which project to the medial septum. Eur J Neurosci 17: 1861–1872.

Ito S, Ishizuka T, Yawo H (2012) Remodeling of hippocampal network in pilocarpine-treated mice expressing synaptopHluorin in the mossy fiber terminals. Neurosci Res 74: 25–31.

Jiao Y, Nadler JV (2007) Stereological analysis of GluR2-immunoreactive hilar neurons in the pilocarpine model of temporal lobe epilepsy: correlation of cell loss with mossy fiber sprouting. Exp Neurol 205: 569–582.

Karoly N, Mihaly A, Dobo E (2011) Comparative immunohistochemistry of synaptic markers in the rodent hippocampus in pilocarpine epilepsy. Acta Histochem 113: 656–662.

Kohler C, Eriksson L, Davies S, Chan-Palay V (1986) Neuropeptide Y innervation of the hippocampal region in the rat and monkey brain. J Comp Neurol 244: 384–400.

Lemos T, Cavalheiro EA (1995) Suppression of pilocarpine-induced status epilepticus and the late development of epilepsy in rats. Exp Brain Res 102: 423–428.

Liu Y, Fujise N, Kosaka T (1996) Distribution of calretinin immunoreactivity in the mouse dentate gyrus. I. General description. Exp Brain Res 108: 389–403.

Longo B, Covolan L, Chadi G, Mello LE (2003) Sprouting of mossy fibers and the vacating of postsynaptic targets in the inner molecular layer of the dentate gyrus. Exp Neurol 181: 57–67.

Longo BM, Mello LE (1997) Blockade of pilocarpine- or kainate-induced mossy fiber sprouting by cycloheximide does not prevent subsequent epileptogenesis in rats. Neurosci Lett 226: 163–166.

Longo BM, Mello LE (1998) Supragranular mossy fiber sprouting is not necessary for spontaneous seizures in the intrahippocampal kainate model of epilepsy in the rat. Epilepsy Res 32: 172–182.

Lurton D, Cavalheiro EA (1997) Neuropeptide-Y immunoreactivity in the pilocarpine model of temporal lobe epilepsy. Exp Brain Res 116: 186–190.

Magloczky Z, Wittner L, Borhegyi Z, Halasz P, Vajda J, Czirjak S, Freund TF (2000) Changes in the distribution and connectivity of interneurons in the epileptic human dentate gyrus. Neuroscience 96: 7–25.

Margerison JH, Corsellis JA (1966) Epilepsy and the temporal lobes. A clinical, electroencephalographic and neuropathological study of the brain in epilepsy, with particular reference to the temporal lobes. Brain 89: 499–530.

Marksteiner J, Ortler M, Bellmann R, Sperk G (1990) Neuropeptide Y biosynthesis is markedly induced in mossy fibers during temporal lobe epilepsy of the rat. Neurosci Lett 112: 143–148.

Mathern GW, Bertram EH, 3rd, Babb TL, Pretorius JK, Kuhlman PA, Spradlin S, Mendoza D (1997) In contrast to kindled seizures, the frequency of spontaneous epilepsy in the limbic status model correlates with greater aber-

rant fascia dentata excitatory and inhibitory axon sprouting, and increased staining for N-methyl-D-aspartate, AMPA and GABA(A) receptors. Neuroscience 77: 1003–1019.

McCarthy JB, Walker M, Pierce J, Camp P, White JD (1998) Biosynthesis and metabolism of native and oxidized neuropeptide Y in the hippocampal mossy fiber system. J Neurochem 70: 1950–1963.

Mello LE, Cavalheiro EA, Tan AM, Kupfer WR, Pretorius JK, Babb TL, Finch DM (1993) Circuit mechanisms of seizures in the pilocarpine model of chronic epilepsy: cell loss and mossy fiber sprouting. Epilepsia 34: 985–995.

Nadler JV, Perry BW, Cotman CW (1980) Selective reinnervation of hippocampal area CA1 and the fascia dentata after destruction of CA3-CA4 afferents with kainic acid. Brain Res 182: 1–9.

Nadler JV, Tu B, Timofeeva O, Jiao Y, Herzog H (2007) Neuropeptide Y in the recurrent mossy fiber pathway. Peptides 28: 357–364.

Nitsch R, Leranth C (1993) Calretinin immunoreactivity in the monkey hippocampal formation--II. Intrinsic GABAergic and hypothalamic non-GABAergic systems: an experimental tracing and co-existence study. Neuroscience 55: 797–812.

Polli RS, Malheiros JM, Dos Santos R, Hamani C, Longo BM, Tannus A, Mello LE, Covolan L (2014) Changes in hippocampal volume are correlated with cell loss but not with seizure frequency in two chronic models of temporal lobe epilepsy. Front Neurol 5: 111.

Rizzi M, Monno A, Samanin R, Sperk G, Vezzani A (1993) Electrical kindling of the hippocampus is associated with functional activation of neuropeptide Y-containing neurons. Eur J Neurosci 5: 1534–1538.

Scharfman HE, Gray WP (2006) Plasticity of neuropeptide Y in the dentate gyrus after seizures, and its relevance to seizure-induced neurogenesis. EXS 95: 193–211.

Scharfman HE, Smith KL, Goodman JH, Sollas AL (2001) Survival of dentate hilar mossy cells after pilocarpine-induced seizures and their synchronized burst discharges with area CA3 pyramidal cells. Neuroscience 104: 741–759.

Seress L, Abraham H, Horvath Z, Doczi T, Janszky J, Klemm J, Byrne R, Bakay RA (2009). Survival of mossy cells of the hippocampal dentate gyrus in humans with mesial temporal lobe epilepsy. J Neurosurg 111: 1237–1247.

Silva JG, Mello LE (2000) The role of mossy cell death and activation of protein synthesis in the sprouting of dentate mossy fibers: evidence from calretinin and neo-timm staining in pilocarpine-epileptic mice. Epilepsia 41 (Suppl 6): S18–23.

Sloviter RS (1987) Decreased hippocampal inhibition and a selective loss of interneurons in experimental epilepsy. Science 235: 73–76.

Sloviter RS (1991) Permanently altered hippocampal structure, excitability, and inhibition after experimental status epilepticus in the rat: the "dormant basket cell" hypothesis and its possible relevance to temporal lobe epilepsy. Hippocampus 1: 41–66.

Sperk G, Marksteiner J, Gruber B, Bellmann R, Mahata M, Ortler M (1992) Functional changes in neuropeptide Y- and somatostatin-containing neurons induced by limbic seizures in the rat. Neuroscience 50: 831–846.

Takacs VT, Freund TF, Gulyas AI (2008) Types and synaptic connections of hippocampal inhibitory neurons reciprocally connected with the medial septum. Eur J Neurosci 28: 148–164.

Terada S, Tsujimoto T, Takei Y, Takahashi T, Hirokawa N (1999) Impairment of inhibitory synaptic transmission in mice lacking synapsin I. J Cell Biol 145: 1039–1048.

Turski WA, Cavalheiro EA, Bortolotto ZA, Mello LM, Schwarz M, Turski L (1984) Seizures produced by pilocarpine in mice: a behavioral, electroencephalographic and morphological analysis. Brain Res 321: 237–253.

Turski WA, Czuczwar SJ, Kleinrok Z, Turski L (1983) Cholinomimetics produce seizures and brain damage in rats. Experientia 39: 1408–1411.

Vezzani A, Michalkiewicz M, Michalkiewicz T, Moneta D, Ravizza T, Richichi C, Aliprandi M, Mule F, Pirona L, Gobbi M, Schwarzer C, Sperk G (2002) Seizure susceptibility and epileptogenesis are decreased in transgenic rats overexpressing neuropeptide Y. Neuroscience 110: 237–243.

Vezzani A, Sperk G (2004) Overexpression of NPY and Y2 receptors in epileptic brain tissue: an endogenous neuroprotective mechanism in temporal lobe epilepsy? Neuropeptides 38: 245–252.

Volz F, Bock HH, Gierthmuehlen M, Zentner J, Haas CA, Freiman TM (2011) Stereologic estimation of hippocampal GluR2/3- and calretinin-immunoreactive hilar neurons (presumptive mossy cells) in two mouse models of temporal lobe epilepsy. Epilepsia 52: 1579–1589.

Winawer MR, Makarenko N, McCloskey DP, Hintz TM, Nair N, Palmer AA, Scharfman HE (2007) Acute and chronic responses to the convulsant pilocarpine in DBA/2J and A/J mice. Neuroscience 149: 465–475.

Xu X, Guo F, He Q, Cai X, Min D, Wang Q, Wang S, Tian L, Cai J, Zhao Y (2014) Altered expression of neuropeptide Y, Y1 and Y2 receptors, but not Y5 receptor, within hippocampus and temporal lobe cortex of tremor rats. Neuropeptides 48: 97–105.

Zhang W, Yamawaki R, Wen X, Uhl J, Diaz J, Prince DA, Buckmaster PS (2009) Surviving hilar somatostatin interneurons enlarge, sprout axons, and form new synapses with granule cells in a mouse model of temporal lobe epilepsy. J Neurosci 29: 14247–14256.